A mathematical model to compute the processing limit speed at laser material processing, assisted by an active gas jet

M. PEARSICĂ[*], C.G. CONSTANTINESCU, M.D. BENȚA[a], C. STRÎMBU, C. MIHAI[a]
"Henri Coandă" Air Force Academy, Electronic Department, 160 Mihai Viteazu St, 500183 Brasov, Romania
[a]*"Transilvania" University, 29 Eroilor St, 500036 Brasov, Romania*

This work is going to show a suitable method of determining a model of the limit processing speed, appropriate to laser material processing assisted by an active gas jet. In this purpose the multivariable regressive functions method was used, considering that process dependent variables as functions of independent ones represent surfaces in variables dimensional space. The most relevant input parameters of materials laser processing are the laser power, the assisting gas pressure, the thickness, and the material nature. An indirect way may be used to determine the processing limit speed, function of temperature distribution in the material. The mathematical model analyzed is based on the heat transfer equation in a homogeneous medium heathen by a laser beam. The theoretical results obtained by using the proposed method were confirmed by the practical ones.

(Received July 5, 2011; accepted September 15, 2011)

Keywords: Laser, Processing limit speed, Regressive function, Heat equation, Temperature distribution

1. Introduction

An essential issue of materials processing with power laser beam [1, 2, 3] is to establish the most propitious speed of action. Limit processing speed (v_L) is the maximum speed, where material breakdown is produced continuously. The goal of limit processing speed mathematical modeling is to establish a computer assisted preliminary technological program, based on algorithms describing the correlation between processing parameters and limit processing speed, in metal materials case.

Limit processing speed as a function of main input parameters of laser cutting process may be obtained based on energy conservation law. An analytical method to determine the limit processing speed was presented by the authors in [4], obtaining relationship:

$$v_L = \frac{\eta_T \cdot A \cdot P_L}{l \cdot g \cdot \rho\left(\bar{c} \cdot \bar{T} + L_l + L_v - \eta_T \cdot \eta_o \dfrac{\varepsilon}{M}\right)} \qquad (1)$$

where: η_T is cutting thermic efficiency; A - surface absorbability; P_L - laser power; g - material thickness; $\bar{c}$ - average specific heat of the material from the slot; $\bar{T}$ - average temperature of the material from the slot; L_l - latent melting heat; L_v - latent heat of vaporization; η_o - oxidizing efficiency; l - average width slot; ρ - metal mass density; M - atomic mass of metal; ε - oxidizing energy on completely oxidized metal atom.

When establishing (1) it was neglected power loss by radiation and convection, and it was considered that all material is evaporated from the slot and all metal atoms in slot volume are completely oxidized. Processing speed dependence on assisting gas pressure, p, is achieved through oxidation efficiency, η_o :

$$\eta_o(p) = erf\left(\frac{p}{p_o}\right) = \frac{2}{\sqrt{\pi}}\int_0^{\frac{p}{p_o}} e^{-u^2} du \qquad (2)$$

where $p_o = 1bar$. This relationship approximates the processing speed variation vs. assisting gas pressure.
Dependence of processing speed on assisting gas pressure, was introduced in (1) through the function $erf(x)$. It was noted that assisting gas pressure between *2...4 bar* leads to achieve maximum efficiency of processing [5], and $erf(p/p_0) \cong 1$.

In (1) the material constants of Fe and estimated (on the basis of research) $\bar{c}$, $\bar{T}$ and η_T are replaced by: $\rho = 7{,}8 \cdot 10^3 kg/m^3$; $\eta_T = 0{,}7$; $M = 9{,}3 \cdot 10^{-26} kg$; $\varepsilon = 9{,}24 \cdot 10^{-19} J$; $\bar{T} = 6680K$; $\bar{c} = 790 J \cdot kg^{-1} \cdot K^{-1}$; $L_l = 273 \cdot 10^3 J/kg$; $L_v = 6073 \cdot 10^3 J/kg$ [6].
It results:

$$v_L = 4{,}62 \frac{P_L\ [W]}{g\ [mm]}\ [mm/min] \qquad (3)$$

The relationship obtained for calculating the limit speed is suitable for steels with high iron content, using oxygen as assisting gas, its pressure being between *2...4 bar*. Processing speed optimization has been experimentally achieved. Following these experimental researches performed on various types of materials, imposing to get a slot width *l* and a tapered low rate, it was determined laser beam processing speed for varying parameters P_L, *g* and *p*. In this purpose it was use the multivariable regression functions method [7], considering the dependences between dependent and independent variables of a process as (hyper) surfaces in variables space.

2. Evaluation of laser processing speed depending on the temperature distribution

An indirect way may be used to determine a more precise processing limit speed, function of temperature distribution in the material [8, 9, 10]. The mathematical model is based on the heat transfer equation, into a homogeneous material, laser beam heated. Because transient phenomena are discussed, it is necessary to consider simultaneously the three phases in material (solid, liquid and vapor), these implying boundary conditions for unknown boundaries, resulting in this way analytical and numerical approach with high complexity [11, 12, 13].

The main hypothesis basing the mathematical model elaboration, derived from previous research team achievements [11, 14, 15], are: laser processing is a consequence of photon energy transferred in the material and active gas jet, increasing the metal destruction process by favoring exothermic reactions; the processed material is approximated as a semi-infinite region, which is the space limited by the plane $z = 0$, the irradiated domain being much smaller than substance volume; the power laser beam has a “Gaussian” type radial distribution of beam intensity (valid for TEM_{00} regime); laser beam absorption at *z* depth respects the Beer law; oxidations occurs only in laser irradiated zone, oxidant energy being “Gaussian” distributed; the attenuation of metal vapors flow respects an exponential law. One of the mathematical hypothesis needing a deeper analysis is the shape of the boundaries between liquid and vaporization, respectively liquid and solid states, supposed as previously known, the parameters characterizing them being computed in the thermic regime prior to the calculus moment.

Regarding the working regime, two kinds of lasers were taken into consideration: continuous regime lasers and pulsated regime lasers (P_L has periodical time dependence, governed by a “Gaussian” type law). If the laser pulse period is $t_p = t_{on} + t_{off}$, then the expression used for the laser power is the following:

$$P_L = \begin{cases} C\left[e^{-\frac{1}{4}} - e^{-\left(\frac{t - \frac{t_{on}}{2} - k t_p}{t_{on}}\right)^2}\right], & t \in \left[k t_p,\ k t_p + t_{on}\right] \\ 0, & t \in \left((k+1)t_p - t_{off},\ (k+1)t_p\right) \end{cases} ;\ k \in N \quad (4)$$

where: $C = P_{L\,max} \cdot e^{1/4}$.

The power flow on the processed surface corresponding to vapor state is given by [11]:

$$\varphi_V(M,t) = C_G \cdot e^{-\left(\frac{r}{d_V}\right)^2},\quad r^2 = x^2 + y^2,\ z = z_f \quad (5)$$

where: $C_G = C_{G_1} + C_{G_2} = \frac{P_L}{\pi d_V^2} + \frac{\eta_o \cdot \varepsilon \cdot \rho_v \cdot v_S}{M}$ (d_V - radius of the laser beam on the separation boundary between vapor state and liquid state and it is calculated with (6), z_f - z coordinate corresponding to the boundary between vapor state and liquid state; C_{G_2} is considered only in the vapor state, because the vaporized metal diffusing in atmosphere suffers an exothermic air oxidation, thus resulting an oxidizing energy which provides supplemental heating of the laser beam processed zone).

$$d_V = d + \frac{D - d}{f} \cdot z_f \quad (6)$$

where: D is the diameter of the generated laser beam and f is the focusing distance of the focusing system.

As a result of laser beam action, the processed material surface heats, its temperature reaching the melting value, T_{top} at a certain moment of time. The heating goes on, so in another moment of time, the melted material temperature reaches the vaporization value, T_{vap}. That moment onward the vapor state appears in material. The equations (7), (8), (9), and (10) still govern the heating process in all of three states (solid, liquid and vapor), changing the material constants *k* and *K*, which will be denoted according to the state of the point *M(r,z)*, as it follows: k_1, K_1 - for the solid state, k_2, K_2 - for the liquid state, respectively k_3, K_3 - for the vapor state [11, 14].

$$\frac{1}{K}\frac{\partial T}{\partial t} = \frac{1}{r}\frac{\partial T}{\partial r} + \frac{\partial^2 T}{\partial r^2} + \frac{\partial^2 T}{\partial z^2} \quad (7)$$

$$T(r,z,0) = T_a,\quad (r,z) \in [0,\ r_\infty] \times [0,\ r_\infty] \quad (8)$$

$$\frac{\partial T(r,0,t)}{\partial z} = \begin{cases} -\frac{1}{k}\varphi(r,0,t), & r \le d \\ 0, & r > d \end{cases} \quad (9)$$

$$T\left(r_{\infty},z,t\right)=T_{a}, \quad z>0 \tag{10}$$

where: K is the diffusivity, and k - heat conductivity of the material.

The three states are separated by time varying boundaries. To know these boundaries is essential to determine the thermic regime at a certain time moment. If the temperature is known, then the following relations describe the boundaries separating the processed material states:

- solid and liquid states boundary:

$$T\left(r,z,t\right)=T_{top}, \quad \left(r,z\right)\in C_{l}\left(t\right) \tag{11}$$

- liquid and vapor states boundary:

$$T\left(r,z,t\right)=T_{vap}, \quad \left(r,z\right)\in C_{v}\left(t\right) \tag{12}$$

The material temperature rises from T_{top} to T_{vap} between the boundaries $C_l(t)$ and $C_v(t)$.

The first step of the mathematical approach is to make the equations dimensionless. In heat equation case it will be achieved by considering the following (r_∞ and z_∞ are the studied domain boundaries, where the material temperature is always equal to the ambient one):

$$r=x\,r_{\infty}, \quad z=y\,r_{\infty}, \quad T=T_{a}\,u, \quad t=\frac{r_{\infty}^{2}}{K_{1}}\tau \tag{13}$$

The heat equation in the new variables x, y, τ, and u yields:

$$\frac{1}{x}\frac{\partial u}{\partial x}+\frac{\partial^{2}u}{\partial x^{2}}+\frac{\partial^{2}u}{\partial y^{2}}=\frac{K_{1}}{K_{i}}\frac{\partial u}{\partial \tau}, \quad \left(x,y\right)\in\left[0,1\right]\times\left[0,1\right] \tag{14}$$

Using the finite differences method, the domain $[0,1]\times[0,1]$ is digitized by sets of equidistant points on Ox and Oy directions.

The equations system obtained after digitization and boundary determination were solved [10] by using an optimized method regarding the solving run time, namely the column wise method. It is an exact type method, preferable to the direct matrix inversing method.

The model equations were solved for a cutting process of metals with a high concentration of iron (steel case).

The input data are: $P_L = 1\,kW$, $\eta_o = 0.74$, $p = 0.8\,bar$, $d = 0.16\,mm$, $D = 10\,mm$, $f = 145\,mm$, $g = 6\,mm$, $t = 10\,ms$ (operation time). The iron material constants were taken into consideration, accordingly to the present (solid, liquid or vapor) state.

Temperature distribution, computed in continuous regime lasers, is represented in two situations: at the material surface and at the material evaporating depth $\left(z = 4{,}192\,mm\right)$.

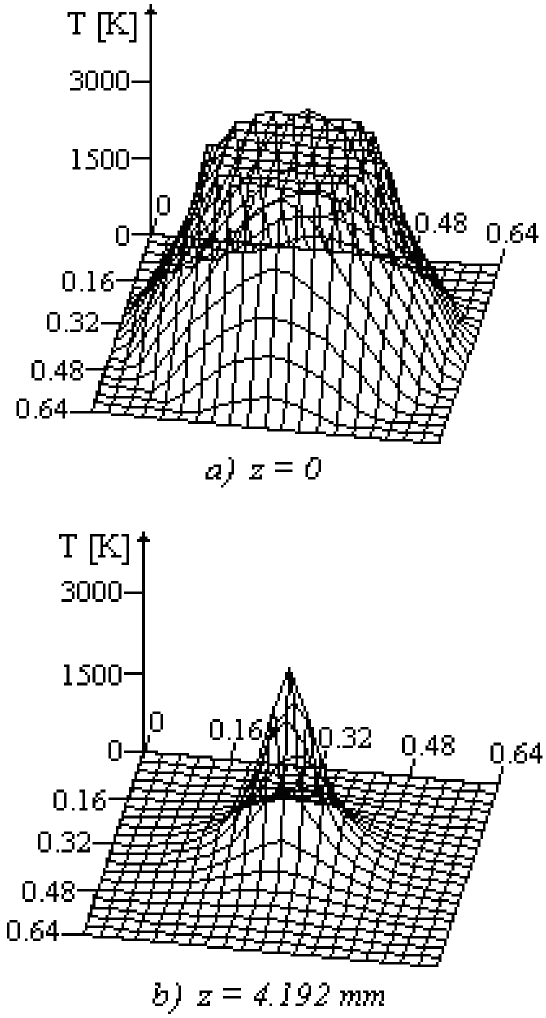

Fig. 1. Temperature distribution.

The depths corresponding to the melting and vaporization temperatures are: $z_{top} = 4.288\,mm$, respectively $z_{vap} = 4.192\,mm$. The moments when material surface reaches the vaporization and melting temperatures are: $t_{vap} = 0.181\cdot10^{-5}\,s$, respectively $t_{top} = 0.132\cdot10^{-5}\,s$. Material vaporization depth is depending on the processing time, and the considered input parameters as well. Knowing the vaporization depth at a certain processing time allows evaluating the vaporization speed and limited processing speed.

The processing speed is computed for a certain material thickness, as a function of vaporization speed (v_{vap}) corresponding to processing moment when vaporization depth is equal to material thickness. So, for a certain processing time, results the thickness of the material that may be processed, which is equal to vaporization depth.

Because of the mass-flow conserving law, in order to cut a material with a certain thickness, the time requested by moving the irradiated zone must be equal to the time requested by material breakdown. The following relation derives in this way, allowing evaluating the processing speed as a function of vaporization speed:

$$v_L = v_{vap} \cdot \frac{2d}{g} \tag{15}$$

The variations of processing speed as functions of material thickness are represented for two pressures of assisting gas (*0.8bar*, *3bar*).

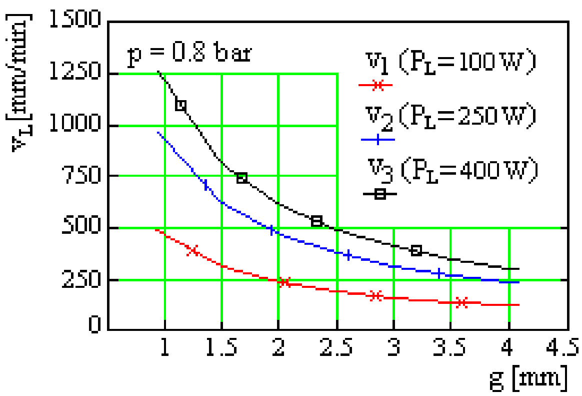

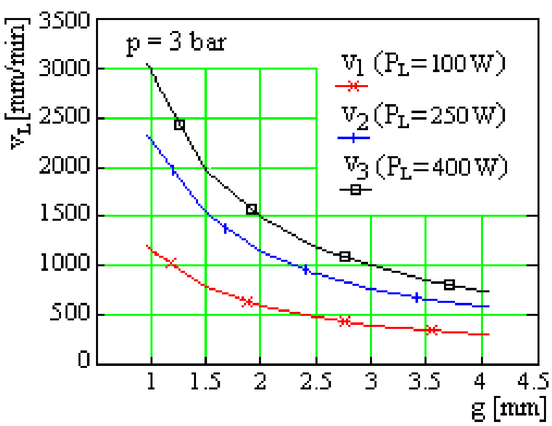

Fig. 2. The processing speed variation vs. material thickness.

It may be observed that processing speed is a decreasing function related to material thickness and an increasing one related to laser power and assisting gas pressure.

3. Multivariable regressive function method

The most relevant input parameters (independent variables) of laser beam processing are: the laser power $P_L[W]$, the active gas pressure $p[bar]$, the type and material thickness $g[mm]$.

The determination of a regression function implies certain problems like: to establish the function form and the experimental program structure, to calculate the regression coefficients, the regression analysis, to determine the statistic errors and the confidence interval for the dependent variable [4].

The regression process function, which is going to be determined, is:

$$y = f(x_1, x_2, x_3) = a_0\, x_1^{a_1}\, x_2^{a_2}\, x_3^{a_3} \overset{ln}{\Rightarrow} \tag{16}$$

$$Y = \ln a_0 + \sum_{j=1}^{3} a_j z_j \tag{17}$$

where: $y = v_L$; $x_1 = P_L$; $x_2 = p$; $x_3 = g$; $Y = \ln y$; $z_j = \ln x_j$; $j = 1,2,3$.

It will use the least squares method [16], so that the deviation function becomes:

$$G(a_0, a_1, a_2, a_3) = \sum_{i=1}^{n}\left(Y_i - \ln a_0 - \sum_{j=1}^{3} a_j z_{j_i} \right)^2 \tag{18}$$

where n is the number of different experiments, and $z_{j_i} = \ln x_{j_i}$, x_{j_i} being the value of independent variable x_j in i^{th} experiment. By nullifying the partial derivatives of G related to $\ln a_0$, a_1, a_2 and a_3, it results the normal equations system:

$$\begin{cases} m \cdot \ln a_0 + \sum_{j=1}^{3} a_j \cdot \sum_{i=1}^{n} z_{ji} = \sum_{i=1}^{n} Y_i \\ \sum_{i=1}^{n} z_{1_i} \cdot \ln a_0 + \sum_{j=1}^{3} a_j \cdot \sum_{i=1}^{n} (z_{j_i} \cdot z_{1_i}) = \sum_{i=1}^{n} (Y_i \cdot z_{1_i}) \\ \sum_{i=1}^{n} z_{2_i} \cdot \ln a_0 + \sum_{j=1}^{3} a_j \cdot \sum_{i=1}^{n} (z_{j_i} \cdot z_{2_i}) = \sum_{i=1}^{n} (Y_i \cdot z_{2_i}) \\ \sum_{i=1}^{n} z_{3_i} \cdot \ln a_0 + \sum_{j=1}^{3} a_j \cdot \sum_{i=1}^{n} (z_{j_i} \cdot z_{3_i}) = \sum_{i=1}^{n} (Y_i \cdot z_{3_i}) \end{cases} \tag{19}$$

System matrix determinant is:

$$V = \begin{vmatrix} n & \sum_{i=1}^{n} z_{1_i} & \sum_{i=1}^{n} z_{2_i} & \sum_{i=1}^{n} z_{3_i} \\ \sum_{i=1}^{n} z_{1_i} & \sum_{i=1}^{n} (z_{1_i})^2 & \sum_{i=1}^{n} (z_{1_i} \cdot z_{2_i}) & \sum_{i=1}^{n} (z_{1_i} \cdot z_{3_i}) \\ \sum_{i=1}^{n} z_{2_i} & \sum_{i=1}^{n} (z_{2_i} \cdot z_{1_i}) & \sum_{i=1}^{n} (z_{2_i})^2 & \sum_{i=1}^{n} (z_{2_i} \cdot z_{3_i}) \\ \sum_{i=1}^{n} z_{3_i} & \sum_{i=1}^{n} (z_{3_i} \cdot z_{1_i}) & \sum_{i=1}^{n} (z_{3_i} \cdot z_{2_i}) & \sum_{i=1}^{n} (z_{3_i})^2 \end{vmatrix} \tag{20}$$

It may observe a symmetrical system matrix; also it's obvious that the line j elements (general terms of corresponding sums) are derived from those of the first line, multiplying them by v_{0j} item. The free terms vector is:

$$U = \begin{vmatrix} \sum_{i=1}^{n} Y_i \\ \sum_{i=1}^{n} (Y_i \cdot z_{1_i}) \\ \sum_{i=1}^{n} (Y_i \cdot z_{2_i}) \\ \sum_{i=1}^{n} (Y_i \cdot z_{3_i}) \end{vmatrix} \quad (21)$$

The unknown vector yields immediately:

$$A = V^{-1} \cdot U \quad (22)$$

The structure of the experimental research program, used to determine the regression coefficients, includes the following elements: n - number of different experiments, required by regression coefficients determination; n_o - number of identical experiments, required by experimental errors determination; x_j^u - levels, respectively the values of the variables x_j, $j = 1,2,3$, effectively experimented; $u = 1,2,...,N$ - variation levels; E_i, $i = 1,2,...,n_t$ - experiments content,

$$E_i = \{ w_{i1}, w_{i2}, w_{i3} \}, \quad i = 1,2,..., n_t \quad (23)$$

where w_{ij} is the level of x_j variable at i experience, and n_t is the entire amount of experiments program.
Working with 3 levels ($N = 3$) for each variable, the minimum, medium and maxim codified levels will be: –1, 0, and respectively +1. In order to cover the experimental area bordered by the limits of the variables variation intervals, the minimum level x_{jmin} and maximum one x_{jmax} will be considered equal to the limits of the respective intervals, and the medium x_{jmed} will be:

$$x_{jmed} = \sqrt{x_{j\,min} \cdot x_{j\,max}}, \quad j = 1,2,3 \quad (24)$$

The experimental research program used for regression functions determination is presented in Table 1 (P_1 type) [4].

Table 1. Structure of experimental research program.

Structure (P_1 program)							Number of regression coefficients (m + 1)
x_j \ i	1	2	3	4	5	6	
x_1	+1	–1	–1	+1	0	0	4
x_2	–1	+1	–1	+1	0	0	
x_3	–1	–1	+1	+1	0	0	

The regression analysis includes checking up of the adequacy of the regression function form and of the regression coefficients significance. In purpose of obtaining an adequate model, it is necessary that the inadequacy index R^* should be subunit:

$$R^* = \frac{F^*}{F(n - n_o - m, n_o - 1, P)} < 1 \quad (25)$$

where: F represents statistics of Fisher repartition; P - probability ($P = 95\%$); F^* - the ratio between the inadequacy square average and the square average of experimental errors.

In order to check up the significance of the regression coefficients, it must define the significance index R_j of the coefficient a_j:

$$R_j = \frac{F_j}{F(1, n - m - 1, P)}, \quad j = 0,1,2,...,m \quad (26)$$

where: F_j has a Fisher repartition and it is the ratio between the square average of the coefficients and the square average of the residues. The regression coefficient a_j is significant if $R_j > 1$.

The statistics errors represent the absolute or relative differences between the measured responses and those calculated and they give a suggestive image of the description of the studied process by the determined regression function.

4. Experimental results

To check experimentally the limit processing speed with laser beam assisted by a gas jet (3) in case of materials with high content of Fe, it was determined experimentally as function of process independent variables: P_L - laser power, g - material thickness and, p - work gas pressure.

Experimental determination of limit speed for laser beam processing steels, assisted by an active jet gas, were fulfilled with EUROLAS 1502 laser installation. The installation includes a CO_2 laser from TRIAGON series, with a power control range of: *0…3000W d.c.* Materials used as probes were from plain steel (OL37), alloy steel (15Cr08) and stainless steel (12Cr130) categories. The experiments program (Table 2) for processing limit speed (v_L) was established taking into account the experimental methodology.

Table 2. Experiments program for processing limit speed.

x_j		Processed material			Y
		OL37	15CR08	12CR130	$P_1(4)$
P_L *[W]*	-1	2000	2000	1400	v_L *[mm/min]*
	0	2450	2450	1980	
	+1	3000	3000	2800	

p *[bar]*	-1	0,8	0,8	15	
	0	1,6	1,6	17,3	
	+1	3,2	3,2	20	
g *[mm]*	-1	4	4	1	
	0	6,9	6,9	2	
	+1	12	12	4	

According to all independent levels of processing regime, the average was calculated so that the minimum, average and maximum level, in natural units, to be in geometric progression. The experimental results for processing limit speed (v_L) according to the processed material are presented in Table 3.

Table 3. Experimental results.

Exp.	Experimental results v_L *[mm/min]*		
	OL37	15Cr08	12Cr130
1	2860	2320	8960
2	2190	2120	5350
3	920	780	1120
4	1640	1460	2480
5	1780	1650	3070
6	1890	1690	3160

For each experience in the program, it has worked continuously on a length of about 100mm, imposing a maximum width of the processing not greater than $250\,\mu m$. The aim was to obtain constant and reproducible process parameters, is performed measurements of gap size and shape and quality of processed surface. Each experience of the program was carried out several times, varying the processing speed within $700...8960\, mm / min$ and selecting the maximum processing speed, which allows to get constant and reproducible parameters with imposed limit values.

Samples were scanned with laser profilometry $NanoFocus\ \mu Scan$, allowing two and three-dimensional measurements without contact processed surfaces microtopography.

Fig. 3 presents the image obtained by using profilometry for 15Cr08 ($v_L = 2120\, mm / min$, $P_L = 2000\, W$, $p(O_2) = 3{,}2\, bar$, $g = 3\, mm$), and figure 4 for 12Cr130 ($g = 4\, mm$, $v_L = 2480\, mm / min$, $P_L = 2800\, W$, $p(N_2) = 20\, bar$).

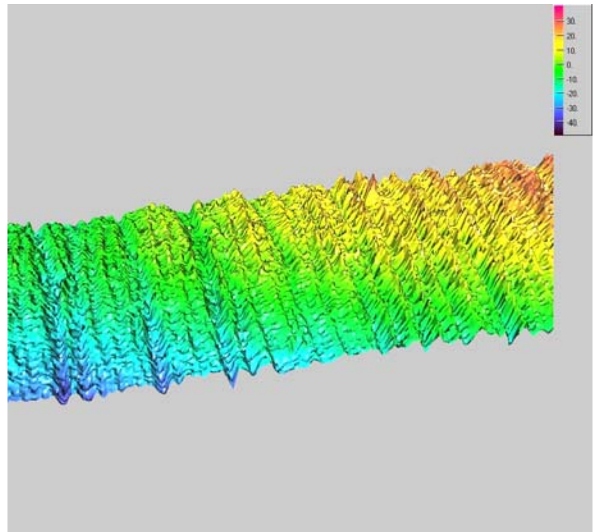

Fig. 3. Capture from profilometer - 15Cr08.

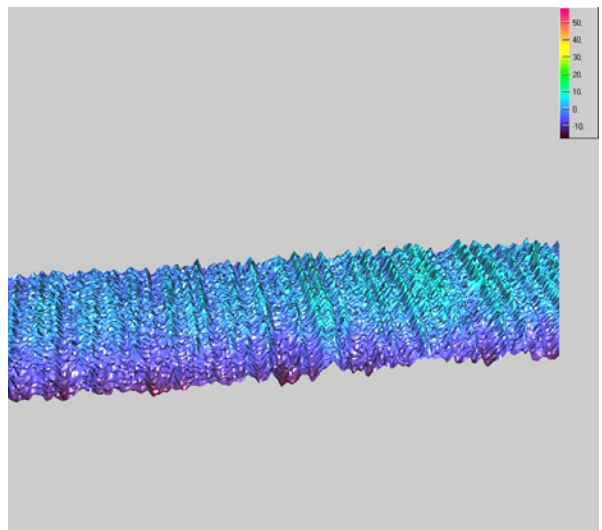

Fig. 4. Capture profilometer - 13Cr130.

Analysis of phenomena that occur at microscopic level and study of structural changes in metallic materials processed with laser beam allows for determining the correlation between laser and material parameters and technological parameters of the processing system. Profile, ripples and roughness of scanned surfaces are presented in the following figures:

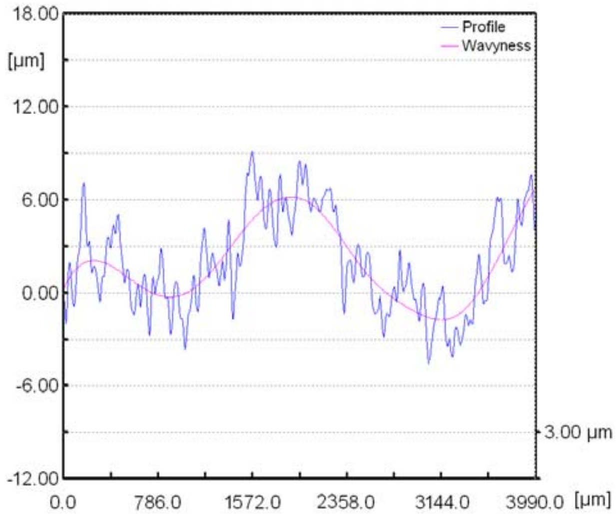

Fig. 5. Profile and ripples - 15Cr08.

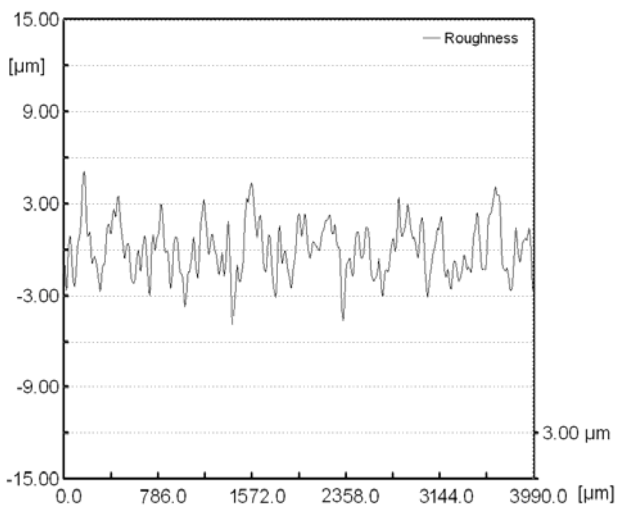

Fig. 6. Roughness - 15Cr08.

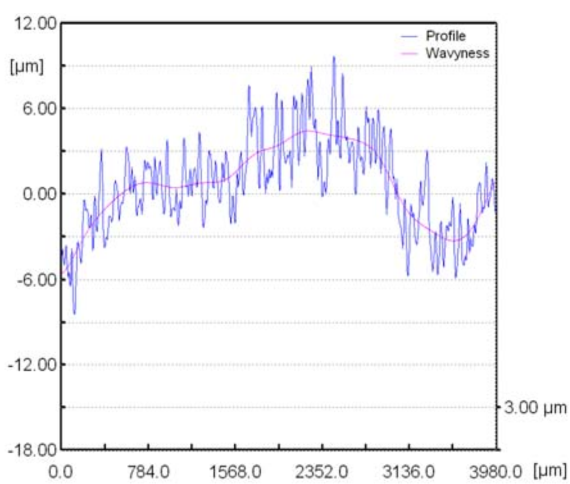

Fig. 7. Profile and ripples - 12Cr130.

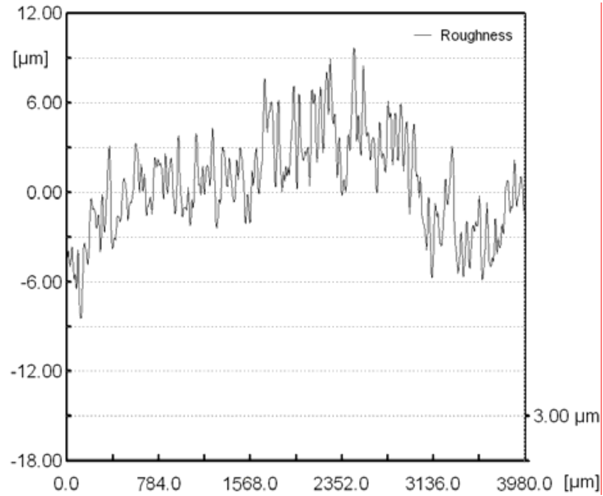

Fig. 8. Roughness - 12Cr130.

From the analysis, it results that the experimentally determined processing speeds depending on the type and thickness, laser power and pressure of gas jet used, the results that are reproducible and within the imposed limits, as well as processing parameters.

Metallographic sample survey was carried out in the Laboratory of Optical Microscopy at the University of Suceava.

5. Experimental modeling of processing limit speed

The data returned by numerical determination are presented in Table 4, for the processed materials types.

Table 4. The regression coefficients.

y	Material	Coefficients a_i			
		a_0	a_1	a_2	a_3
v_L [mm/min]	OL37	0.554	1.042	0.112	−0.648
	15Cr08	1.663	0.884	0.194	−0.666
	12Cr130	0.253	0.945	0.485	−1.027

They result the mathematical equations for regression functions (Table 5):

Table 5. Equations of experimental model.

y	Material	Equations of experimental model
v_L [mm/min]	OL37	$v_L = 1.714 \cdot P_L^{1.042} p^{0.112} g^{-0.648}$
	15Cr08	$v_L = 5.135 \cdot P_L^{0.884} p^{0.194} g^{-0.666}$
	12Cr130	$v_L = 1.326 \cdot P_L^{0.945} p^{0.485} g^{-1.027}$

It results from the mathematic model equations that v_L increases (decreases) exponentially with P_L and p (g).

Regression functions of limit processing speed were represented as response surfaces (Fig. 9, 10 and 11) for OL37, in order to see how working parameters differently affect v_L.

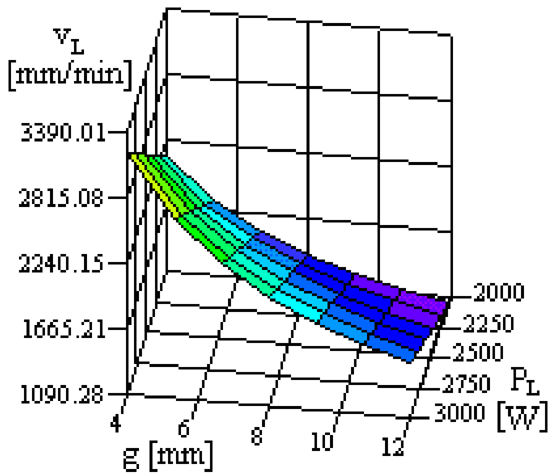

Fig. 9. $v_L = f(P_L, g)$, $p = 2$ *bar.*

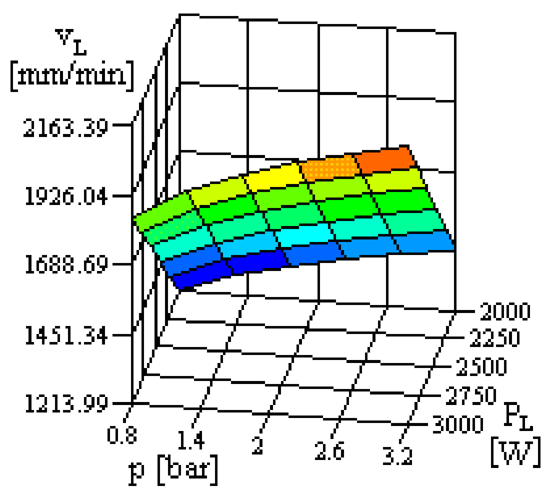

Fig. 10. $v_L = f(P_L, p)$, $g = 8$ *mm.*

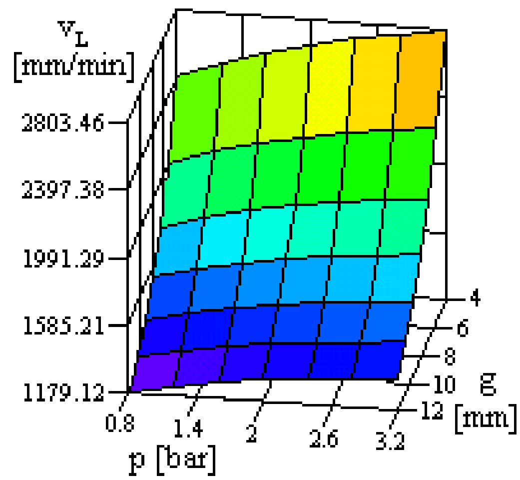

Fig. 11. $v_L = f(g, p)$, $P_L = 2500$ *W.*

For the ranges of parameters considered it observes that: g has a stronger influence compared to P_L (Fig. 9), v_L has an increasing variation with both P_L and p, but the laser power is decisive relating to the working gas pressure (Fig. 10), g, compared to p, has a stronger influence over v_L too (Fig. 11).

The regression analysis results (significance index R_j of the coefficient a_j, inadequacy index R^*, maximum statistic error $\varepsilon_{max}[\%]$) are presented in Table 6.

Taking into account the regression analysis results, we ascertain that the mathematical model used for dependent variable v_L is adequate.

Table 6. Regression analysis results.

Material	R^*	$\varepsilon_{max\%}$	Coefficients significance			
			R_0	R_1	R_2	R_3
OL37	0.009	3.83	8055.33	3.62	0.27	21.45
15Cr08	0.194	6.45	3800.55	1.50	0.84	6.25
12Cr130	0.149	7.49	4072.46	4.44	0.20	20.97

Figs. 12 are showing comparisons between the processing speeds: analytically determined, experimentally determined and returned by the indirect method (processing speed variation vs. temperature distribution in material [4]).

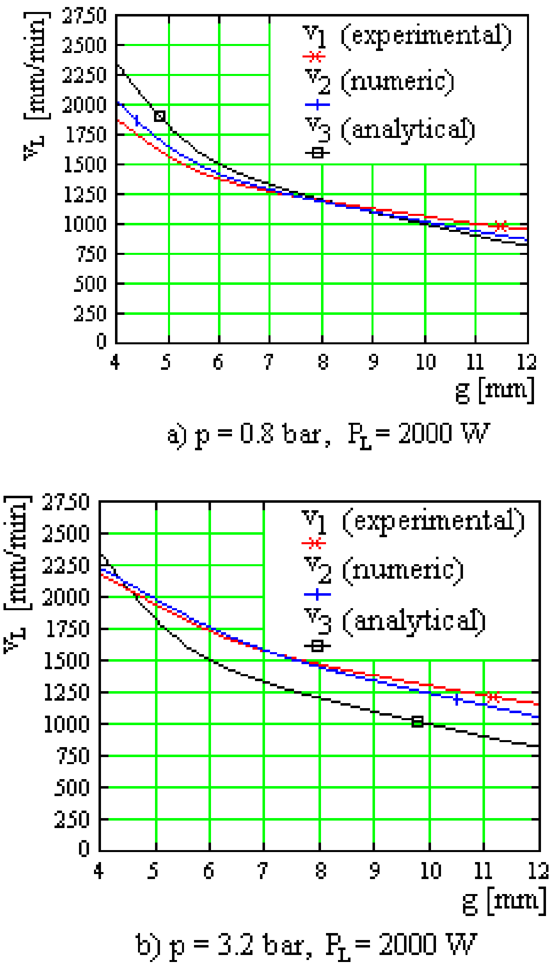

Fig. 9 Limit processing speed comparisons (OL37)

It may be observed in the presented figures that processing speed numerical results are a quite good approximation for the experimental ones, for the laser power $P_L = 2000\ W$, the maximum error being 9.23% for $p = 3.2\ bar$ and, 13.58%, for $p = 0.8\ bar$.

6. Conclusions

Modeling laser processing limit speed (v_L) was achieved by using three methods: an analytical method based on the conservation of energy (3), an indirect method, processing speed being numerically determined function of temperature distribution in material and an experimental modeling method, computing the limit speed as a regression function of the most significant independent variables: P_L, p and g.

The analytical model obtained is experiment dependent, because there are certain difficulties in oxidizing efficiency η_o determination, which implies to model the gas-metal thermic transfer mechanism. As well, some material parameters $(c, k, \rho, A_S,...)$ are temperature dependent.

The method of numeric calculation used to determine the temperature distribution in the material, allows the limit processing speed calculation. The equations of the mathematical proposed model to describe the way the material submitted to laser action reacts were solved numerically by finite differences method. The algebraic system returned by digitization was solved by using an exact type method, known in literature as column solving method. An algebraic system of equation solved at each time-step by column method was obtained after digitization and application of the limit conditions [10, 11]. The procedure is specific to implicit method of solving numerically the heat equation and it was chosen because there were no restrictions on the steps in time and space of the net.

The multivariable regressive function method was applied either to determine the mathematical expression of the limit of processing speed, or to elaborate an experimental mathematical model. The best processing intervals for the laser beam power and active gas pressure were established after the experimental research.

Processing system parameters: laser power (P_L), thickness (g) and working gas pressure (p) differently affect limit processing speed (v_L), as it follows: P_L and g are significant variables, and p in most cases (for $p \geq 1{,}6 bar$) is an insignificant variable.

If assisting gas is a stream of N_2, in case of processing a stainless steel (12Cr130), v_L experimentally determined is higher than the analytical one, because the N_2 jet takes material by erosion, requiring a correction factor in (3) estimated experimental as $f = 1{,}8$.

Limit processing speed limit is influenced by material surface, i.e. its absorbability, structure and thermal parameters, different for each type of material.

According to the presented situation, it may be considered that, in comparison with the analytical processing speed, the numerical determined one match better the experiments. The results thus obtained are within the limits of normal physics, which constitutes a verifying of the mathematical model equation.

Acknowledgements

The National Authority for Scientific Research, Romania supported this work – CNCS-UEFISCDI: Grant CNCS, PN-II-ID-PCE-2008, no 703/15.01.2009, code 2291: "Laser Radiation-Substance Interaction: Physical Phenomena Modelling and Techniques of Electromagnetic Pollution Rejection".

References

[1] J. M. Dowden, The Theory of Laser Materials Processing, Published by Springer, 2008.

[2] J. Perriere, E. Milton, E. Fogarassy, Recent Advaces in Laser Processing Materials, Published by Elsevier, 2006.
[3] W. M. Steen, J. Mazumder, Laser Material Processing, Published by Springer-Verlag, 2010.
[4] C.G. Constantinescu, M. Pearsică, C. Strimbu, M. Benţa, C. Mihai, 9th IASME/WSEAS Int. Conf. – Heat Transfer, Thermal Engineering and Environment, Florence, Italy, August, 208 (2011).
[5] J. F. Ready, LIA Handbook of Laser Materials Processing, Laser Institute of America Magnolia Publishing, Inc., 437, 2001.
[6] V. Draganescu, V. G. Velculescu, Thermal Cutting with Laser Beams, Academy Publishing House, Bucharest, 1986.
[7] C. G. Constantinescu, M. Pearsică, I.G. Ratiu, C. Strimbu, L. Gherman, WSEAS Int. Conf. - New Aspects of Telecommunications and Informatics, Istanbul, Turkey, June, 140 (2009).
[8] I. Belic, Optics and Laser Technology **40**(4), 277 (2008).
[9] L. Hacia, K. Domke, WSEAS Int. Conf. on Heat and Mass Transfer, Athens, Greece, August, 42 (2007).
[10] M. Pearsica, S. Nedelcu, C.G. Constantinescu, C. Strimbu, M. Benta, C. Mihai, Modeling the Physical Phenomena Involved by Laser Beam – Substance Interaction, Heat Transfer – Book 4, INTECH – Open Access Publisher, 2011.
[11] M. Pearsica, I.G. Ratiu, C.G. Carstea, C. Constantinescu, C. Strimbu, L. Gherman, WSEAS Transactions on Mathematics **7**(11), 2174 (2008).
[12] M. Riyad, H. Abdelkader, WSEAS Transactions on Heat and Mass Transfer, **1**(4), 567 (2006).
[13] O.YU. Semchuk, L.G. Grechko, L.B. Lerman, M. Karlsteen, M. Willander, J. Optoelectron. Adv. Mater. **12**(3), 586 (2011).
[14] M. Pearsica, S. Baluta, C.G. Constantinescu, C. Strimbu, J. Optoelectron. Adv. Mater. **10**(5), 2174 (2008).
[15] M. Pearsica, I. G. Ratiu, C.G. Carstea, C. G. Constantinescu, C. Strimbu, Proceedings of the 10th WSEAS Int. Conf. on Mathematical Methods, Computational Technique and Intelligent Systems, Corfu, Greece, October 2008.
[16] L. Rumşiski, Mathematical processing of experimental data, Tehnica Publishing House, Bucureşti, 1972.

*Corresponding author: marianpearsica@yahoo.com